ELSEVIER

Biophysical Chemistry 89 (2001) 129–144

Biophysical Chemistry

www.elsevier.nl/locate/bpc

Molecular characterization of a laminin-derived oligopeptide with implications in biomimetic applications

Solomzi A. Makohliso[a,1], Simone Melchionna[b,*]

[a] *Centre for Gene Therapy, Centre Hospitalier Universitaire Vaudois, CH-1011, Lausanne, Switzerland*
[b] *Department of Chemistry, University of Cambridge, Lensfield Road, CB2 1EW, Cambridge, UK*

Received 15 May 2000; received in revised form 16 October 2000; accepted 16 October 2000

Abstract

The molecular properties of the laminin-derived oligopeptide, H-CDPGYIGSR-NH_2, have been investigated with the aid of a tandem computer simulation/experimental approach. The simulation studies placed a particular emphasis on studying the oligopeptide in aqueous media, as well as in a grafted or immobilized state. The simulations revealed the presence of a stable double hydrogen bond between arginine (R) and aspartic acid (D) residues. The mutation of the terminal arginine with lysine, another hydrophilic and positively charged amino acid, resulted in a drastic structural change, thus suggesting a major role of the terminal arginine residue in the overall oligopeptide's conformation and, hence, its bioactivity. In addition, the involvement of the aspartic acid residue in overall peptide structural stabilization also illustrates a previously undetermined role for this region (i.e. CDPG) of the oligopeptide. A subsequent in vitro experiment demonstrated a significant loss of bioactivity upon mutating the terminal residue from arginine to lysine, thereby corroborating the overall findings of the computational model.

Keywords: Molecular dynamics; Oligopeptides; Laminin; Biomaterials; Tissue-engineering; Cell adhesion

* Corresponding author. Tel.: +44-1223-336350; fax: +44-1223-336362.
E-mail address: melch@theor.ch.cam.ac.uk (S. Melchionna).
[1] Current address: Laboratory for Physical Chemistry of Polymers & Membranes, Department of Chemistry, Swiss Federal Institute of Technology, CH-1015 Lausanne, Switzerland.

0301-4622/01/$ - see front matter
PII: S0301-4622(00)00223-4

1. Introduction

Laminin is a major component of the extracellular matrix that has been shown to exhibit many biological activities with various cell types, including neuronal cells [1]. The interaction of laminin with several primary and established cell lines derived from the peripheral and central nervous systems, has been shown to result in increased cellular adhesion and neurite outgrowth [1–3]. The identification of active sites on the laminin molecule has led to the availability of synthetic oligopeptide analogs, such as YIGSR-NH_2 and IKVAV-NH_2, which can mimic the bioactivity of the respective domains of their origin [4–6]. These synthetic oligopeptides have found widespread interest in cancer research towards preventing tumor metastasis [7–9]. In recent years, there have been several reports aimed at immobilizing these synthetic fragments on artificial surfaces for the purposes of enhancing the biomaterial performance of these surfaces. Several studies in vitro have demonstrated the capability of the immobilized oligopeptides in stimulating cellular adhesion and spreading on these artificial surface [10–14], and in vivo, they have been reported to enable or enhance peripheral nerve regeneration in rodent models [15].

Despite the extensive applications already documented with these biomolecules, several issues regarding the underlying molecular mechanisms of the reported empirical observations remain to be elucidated. For example, in some of the earlier publications it was reported that the variant pentapeptide YIGSK-NH_2 was considerably less bioactive than YIGSR-NH_2 [5,11]. At face value this result is surprising, since Lys (K) is perhaps the closest naturally occurring amino acid to Arg (R) with regards to structure and properties (both positively charged and hydrophilic) and therefore, one would conceivably predict a less dramatic discrepancy with the substitution of one for the other. However, as several data suggest that this is not the case, and the molecular phenomenon underlying this observation has yet to be addressed, a computer simulation approach may be well suited for gaining additional molecular insight about the oligopeptide systems, as it may provide an opportunity to simulate or explore various scenarios not readily accessible empirically. In particular, if used in conjunction with real world experimental data, its potential utility would be significantly enhanced, as the experimental data would help in fine-tuning the computational model and, in turn, the computational results could also improve future experimental design.

Computer simulation studies of YIGSR-containing sequences have been previously reported [16–18], wherein the inspiration was the potential application of laminin-derived fragments towards developing novel drugs against tumor metastasis. Consequently, the peptide structures were examined only in their free floating form. In addition, these simulation studies were all carried out in vacuum media. Brandt-Rauf et al. [16] and McKelvey et al. [17] studied the pentapeptide YIGSR, whereas Ostheimer et al. [18] studied the nonapeptide CDPGYIGSR, and thus their study bears a closer resemblance to the present one. The central focus of Osteheimer et al. was to explore the role of the central Gly residue by mutating it with D-Ala and L-Ala residues, and by using two dimensional H–H NMR try to resolve the structures with the aid of molecular dynamics simulations. From this work, the authors concluded that the Gly residue had a central role for peptide activity. However, the omission of essential details pertaining to the force field employed, such as the treatment of electrostatics and Van der Waals potential, as well as the neglect of the effect of solvent in their simulations, makes it difficult to draw clear conclusions on the structure and stability of the peptide.

The present study sought to extend these earlier efforts by providing an in-depth characterization of the nonapeptide H-CDPGYIGSR-NH_2, as well as examining the effect of an aqueous medium on peptide structure and stability. In addition, we examined the properties of the peptide when one end was constrained to a rigid surface, thereby mimicking peptide immobilization on a solid surface, an issue of widespread interest in areas such as biomaterials and biosen-

sor development. The choice of water as a solvent is indeed appropriate, since peptide immobilization on solid surfaces is typically carried out in water-based media. Furthermore, water is the most abundant fluid in the body and, therefore, the biological relevance of this choice is also implicit. For comparison, we also studied variations of the terminal sequence YIGSR, believed to be the potent domain of the nonapeptide [5]. In one case, the terminal Arg (R) was replaced with Lys (K), to give H-CDPGYIGSK-NH_2, thereafter also referred to as H-CDPGYIGSK-NH_2. In the other case, the active region (YIGSR) was completely rearranged to give H-CDPGRGSYI-NH_2, and is subsequently referred to as the scrambled peptide.

In order to assess the biological relevance of the results of the simulations, an experimental model was constructed in which the synthetic peptide analogs were immobilized on an artificial surface. One of the observations derived from the simulations indicated that the cysteine end of the peptide was always relatively unhindered, thus probably suggesting that it was available to interact with external surfaces. Cysteine contains a thiol side group, widely documented to have a high affinity for inert metal surfaces like gold and silver [19]. Gold, a commonly used substrate in biosensor technology, was thus chosen as the model surface for peptide immobilization, with the hope of fixing the peptide via the thiol side group of the terminal cysteine. Working towards checking for peptide incorporation onto the gold surfaces, electron spectroscopy for chemical analysis (ESCA), a highly surface sensitive analytical technique, was employed to assess the chemical composition of the surfaces. ESCA is a widely used technique for surface characterization that reports quantitatively the elemental composition and chemical bonding information of the top 10–100 Å of the surface [20]. Biological assays of the modified surfaces were carried out with a neuroblastoma X glioma cell line (NG108). This neural cell line was chosen because it is known to possess an appropriate set of cell surface receptors capable of specifically recognizing the YIGSR-containing motif in laminin [1].

2. Materials and methods

2.1. Computational methods

The molecular dynamics simulations on the peptides were performed by using the general purpose code DLPOLY-2.0 [21] with the amendments known as DLPROTEIN [22] for the simulation of proteins. The force field used for modeling the potential function was the CHARMM22 parameter set in the 'all-atoms' scheme. The CHARMM22 Hamiltonian, consisting of angle bending, dihedral torsional, Coulomb and Van der Waals potential terms, was used in conjunction with constrained bond lengths to model the associative chemical bonds [23]. The constraints were treated by applying the SHAKE numerical procedure with a relative tolerance of 10^{-8} [24].

The water model employed in the simulations was the TIP3P model with constrained intramolecular bond lengths [25]. Periodic boundary conditions were used for the simulated solvated systems in order to achieve a truly bulk system in a cubic simulation box. The peptide systems studied were the free-floating forms of H-CDPGYIGSR-NH_2, H-CDPGYIGSK-NH_2 and the scrambled sequence, i.e. H-CDPGRGSYI-NH_2. In addition, to observe the consequences of immobilizing one end of the peptide, the cysteine end of the H-CDPGYIGSR-NH_2 sequence was chemically bound to a two-dimensional rigid crystal via the sulfur atom of the side chain of terminal Cys residue, thus mimicking a grafted peptide. The number of water molecules used to solvate the various peptide systems was 503 for the free H-CDPGYIGSR-NH_2, 500 for grafted H-CDPGYIGSR-NH_2, 488 for free H-CDPGYIGSK-NH_2 and 496 for free H-CDPGRGSYI-NH_2.

The non-bonding interactions were computed by using a cut-off of 9.5 Å, ensuring a proper energy conservation and stability of the dynamics over long periods. The electrostatics of the system were computed by using the Ewald sum method [26] in the form of the smooth particle mesh Ewald (SPME) numerical method [27]. The convergence parameter of the Ewald sum, alpha, was set to 0.3422, while the SPME scheme was used

with a spline interpolation order of 8, and a number of grid points of $20 \times 20 \times 20$, ensuring a relative energy accuracy of 10^{-5}.

The dynamical trajectories were obtained by integrating the trajectories with the velocity Verlet integration algorithm [26] with an integration time step of 1 fs. Each simulated system was initially equilibrated for 100 ps before storing data for subsequent analysis. The duration of each equilibrium trajectory was 500 ps, and for peptide studies in aqueous media this was extended to 2 ns. The analysis was applied over 2500 frames, with configurations stored every 0.2 ps. The simulations were carried out in the isothermal–isobaric (NPT) ensemble [28], in order to ensure a proper sampling of the configurational space, and equilibration of the investigated systems achieved at a temperature of 300 K and pressure of 1 atm. The NPT thermostatting and piston characteristic times were set to 0.4 and 4.0 ps, respectively.

In addition, the analysis of different structures at zero temperature was carried out to investigate the stability of the H-CDPGYIGSR-NH_2 peptide structures obtained from the molecular dynamics runs at finite temperature. The protocol consisted of heating the system to 2000 K for a transient time of 50 ps. Subsequently, the system was quenched down to 0 K in order to obtain the configurations relative to one of the potential energy minima at zero temperature. The cycle was applied five times in order to collect a sufficient number of minimized structures.

The structural analysis performed here was accomplished by analyzing what is termed the most stable dynamical structure (MSDS) observed over the equilibrium run. The MSDS was obtained by computing the atom-averaged displacement of the peptide from the mean structure vs. time [29]. Once this distance reaches a minimum value, the structure obtained is taken as the MSDS. The configurational distance is known to be a good indicator for following the phase space evolution of folded proteins, and the detection of stable configurations [30]. Other typical analyses subsequently performed include the computation of the gyration radius, end-to-end distance and H-bond formation analysis. A H-bond was detected whenever the distance between acceptor and donor atoms was less than 3.5 Å, and the angle formed by the H atom, the acceptor atom and the donor atom was less than 180°, with a tolerance of 65° [29]. Our choice of the distance and angle tolerances is customarily employed when analyzing simulation results within empirical force fields [29].

The VMD graphics software [31] was utilized for visualizing the simulation structures.

2.2. Oligopeptide substrate fabrication

Gold substrates were prepared by electron-beam or thermal evaporation of high purity gold onto oxidized silicon wafers. Prior to gold evaporation, approximately 50 nm of titanium was deposited to serve as an adhesion promoter to subsequent gold deposition (150 nm). Substrates were stored in fluoroware® containers until further use. Prior to oligopeptide surface immobilization, the wafers were diced into smaller pieces of approximately 1×1 cm or any other convenient size, and then briefly sonicated in pure ethanol (Merck, ACS grade). They would then be immersed into a 0.1-mM solution of oligopeptide in double distilled, deionized water and left at room temperature overnight, followed by a thorough rinse with double distilled, deionized water prior to use. The synthetic oligopeptide used was the laminin-derived sequence H-CDPGYIGSR-NH_2, as well as its sequence variant H-CDPGYIGSK-NH_2 (Anawa, Switzerland). Their reported purity is greater than 95%, as determined by analytical high performance liquid chromatography. Their molecular weights, as analyzed by mass spectroscopy, were 966.1 and 937.99, respectively.

2.3. Electron spectroscopy for chemical analysis

ESCA data were obtained using a PHI Perkin-Elmer 5500 equipped with Mg Kα and Al Kα X-ray sources in a dual anode configuration. All our experiments were carried out with a Mg Kα radiation (1253.6 eV) source operating at 300–350 W and 13–14 kV, with a base pressure no higher than 6×10^{-9} torr during analysis. Spectra were

obtained at a takeoff angle of 20° with respect to the surface, and the analyzed area was approximately 1.2 mm^2. Elemental compositions were determined on the basis of peak areas from C1s, N1s, O1s, and Au4f, at pass energies of 93.9 eV for the survey spectra and 23.5 eV for the high energy resolution (multiplex) scans. The acquisition time was approximately 3 min for the survey spectra and 10 min for the multiplex scans. The binding energy was referenced by setting the C1s hydrocarbon peak to 285 eV. Unmodified gold and peptide-modified gold surfaces were analyzed.

2.4. Cell culture

The mouse-derived neuroblastoma X glioma hybrid cell line (NG108-15) was utilized for assessing bioactivity of the synthetic substrates, since it is known to have receptors for the laminin-derived CDPGYIGSR motif. Typically, the cells were cultured in Dulbecco's modified Eagle's medium (DMEM) supplemented with 10% fetal calf serum (FCS), hypoxanthine, aminopterin, thymidine (HAT), penicillin G (100 U/ml) and streptomycin (100 μm/ml) (P/S). In the case of short-term serum-free studies, FCS was simply omitted.

2.5. Biological assays

The model used for our biological essays was adapted from earlier published work [11,12]. In order to check if the CDPGYIGSR-modified substrates elicited any bioresponse, specifically with respect to affecting cell attachment, NG108 cells were cultured at a density of approximately 5×10^4 cells/ml in serum-containing media, on CDPGYIGSR-modified and on unmodified substrates, as control. A minimum of three substrates were used for each substrate type. After 24 h, the culture media was exchanged with a fresh one and this procedure was repeated approximately three times in order to ensure complete removal of floating/unattached cells. With the aid of a grid objective fitted into the microscope, the quantification of cell attachment densities was achieved by counting the number of attached cells observed under each viewing field at a magnification of $160\times$. For each substrate, five random fields were selected. The Student's *t*-test was used to assess statistical significance ($P < 0.05$) for all attachment assays.

In the next experiment, a competitive assay was performed, to test indirectly if the changes observed in cell adhesion events in the preceding experiment might indeed involve the cell's surface receptors. Towards this end, a portion of the harvested cells (group A) were pre-incubated for approximately 2 h, in a serum-free culture medium into which the CDPGYIGSR peptide was also added (0.1 mg/ml) and, thus, was available to the cells in soluble form. The rest of the harvested cells (group B) were treated similarly, except that the soluble peptide was not included in the media during the pre-incubation period. The cells from group A were subsequently plated on CDPGYIGSR-modified surfaces, and the cells from group B were also plated on CDPGYIGSR-modified, as well as on unmodified surfaces, and all these surfaces were subsequently assessed for cell attachment levels (as described above) after 4 h.

In the final experiment, cell attachment levels on CDPGYIGSK-modified surfaces were compared to the CDPGYIGSR surfaces in serum-free media.

The data obtained in the bioassay experiments were analyzed for statistical significance using the Student's *t*-test.

3. Results

3.1. Structure and stability of computed oligopeptides in vacuo

A cross comparison of the MSDS of the two peptides shows that, in general, H-CDPGYIGSR-NH_2 has a more open structure (Fig. 1, left) than H-CDPGYIGSK-NH_2 (Fig. 1, right). Analysis of the computed MSDS shows that the H-CDPGYIGSR-NH_2 peptide has a very strong tendency to sit in a stable configuration in which the terminal Cys residue is unhindered, with the sulfur atom from its side chain exposed (Fig. 2). The terminal Arg residue also seems unhindered

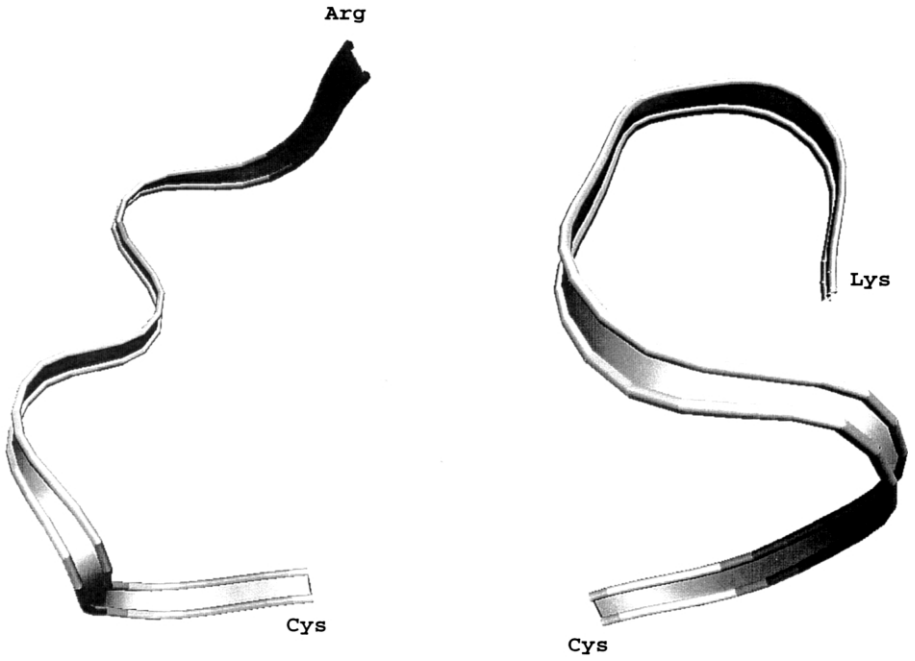

Fig. 1. The representative backbone structure of the most stable dynamic structure (MSDS) of the oligopeptides H-CDPGYIGSR-NH_2 (left) and H-CDPGYIGSK-NH_2 (right) simulated in vacuum. The overall structure of H-CDPGYIGSR-NH_2 is an open, M-shaped structure. In contrast, the structure of H-CDPGYIGSK-NH_2 is somewhat closed or more compact, displaying an S-shaped overall structure. However, note that in both peptides Cys residue is freely exposed.

and available to interact with its surrounding environment. The structure of H-CDPGYIGSK-NH_2, on the other hand, shows (as in H-CDPGYIGSR-NH_2) an exposed sulfur atom from Cys, but a more compact overall structure (Fig. 3). In addition, the side chain residue of Lys displays a marked tendency to fluctuate in space.

The picture is further clarified by looking at H-bond formation and stability. In general, the H-CDPGYIGSR-NH_2 peptide has more intramolecular H-bonds forming over time, with an average of nine H-bonds per configuration, in comparison to H-CDPGYIGSK-NH_2, whose corresponding average is 5.5 H-bonds. A closer look at the H-bond pattern formation during the simulation of H-CDPGYIGSR-NH_2 showed a stable double H-bond shared between the carboxylic group of Asp, where the two oxygens are the acceptors, and the two terminal amino groups of Arg, where the nitrogens act as donors. This double H-bond is practically unbroken over the whole simulation run (Fig. 2, right). On the contrary, the H-CDPGYIGSK-NH_2 system showed a predominant single H-bond between the oxyphilic group of Ser (acceptor) and the terminal amino group of Lys (donor). Furthermore, H-CDPGYIGSK-NH_2 also displays a weak single H-bond between the carboxylic group of Asp and the amino side chain group of Lys.

3.2. Structure and stability of computed oligopeptides in solvent

The stability of the peptides (free H-CDPGYIGSR-NH_2, grafted H-CDPGYIGSR-NH_2, free H-CDPGYIGSK-NH_2 and free H-CDPGRGSYI-NH_2) in solution was initially assessed by computing their radii of gyration, and their respective H-bond formation tendencies. The three peptide systems, viz. free H-CDPGYIGSR-NH_2, grafted H-CDPGYIGSR-NH_2 and the scrambled sequence generally dis-

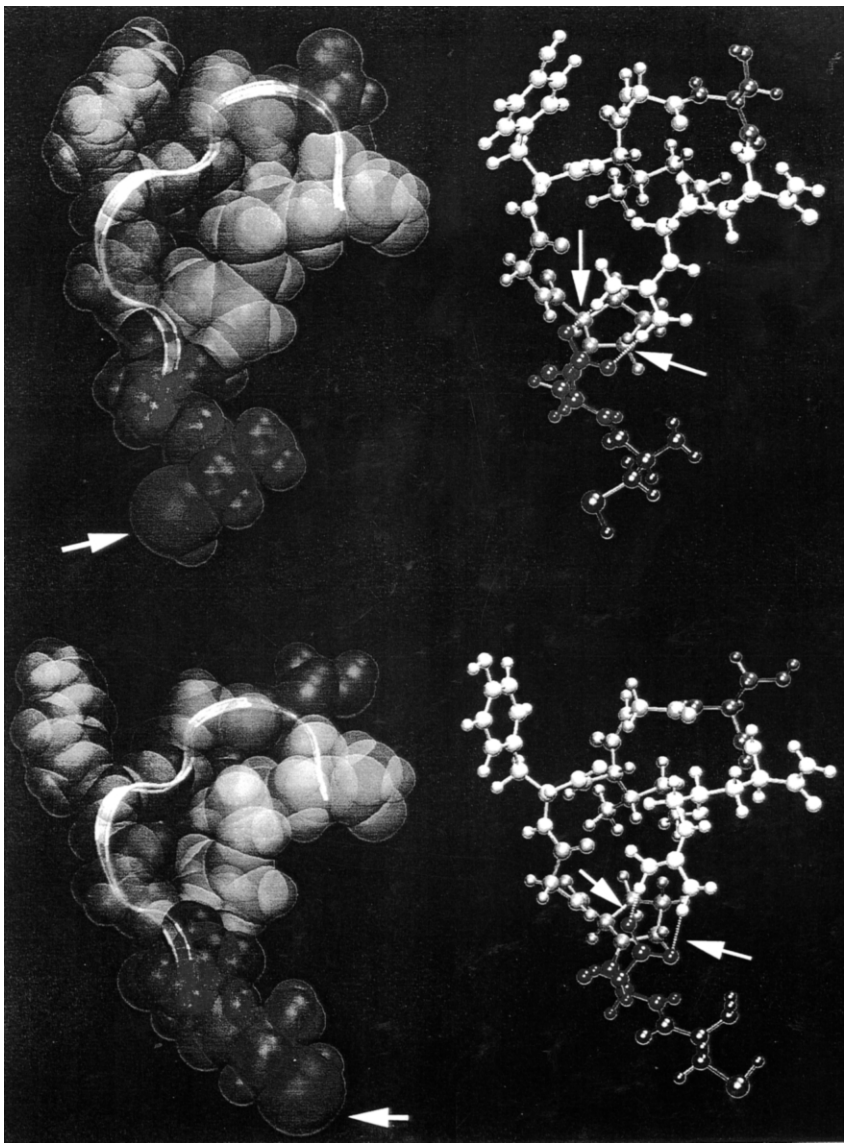

Fig. 2. H-CDPGYIGSR-NH_2 simulated in water in the free (top half) and immobilized/grafted (bottom half) states. On the left hand side are the space-filling models in transparent mode, on which the representative backbone ribbon structures are superimposed. The freely exposed sulfur atom of Cys is indicated at the bottom of each drawing with a white arrow. On the right hand side are ball-and-stick models which also depict the enduring double hydrogen bond (yellow arrows) between Arg and Asp residues. Note the similarity between the structures of the free and immobilized oligopetides. Furthermore, the backbone structure also displays close similarity (M-shape) to the one in vacuum (Fig. 1). Graphics obtained with VMD package [31].

played an open structure and similar radii of gyration, whereas H-CDPGYIGSK-NH_2 seemed to adopt a more closed overall shape and generally more stable structure. The H-CDPGYIGSR-NH_2 molecule behaved in a very similar fashion whether it was in a free or grafted form, with respect to the extent of fluctuations undergone and molecular size, displaying an average radius

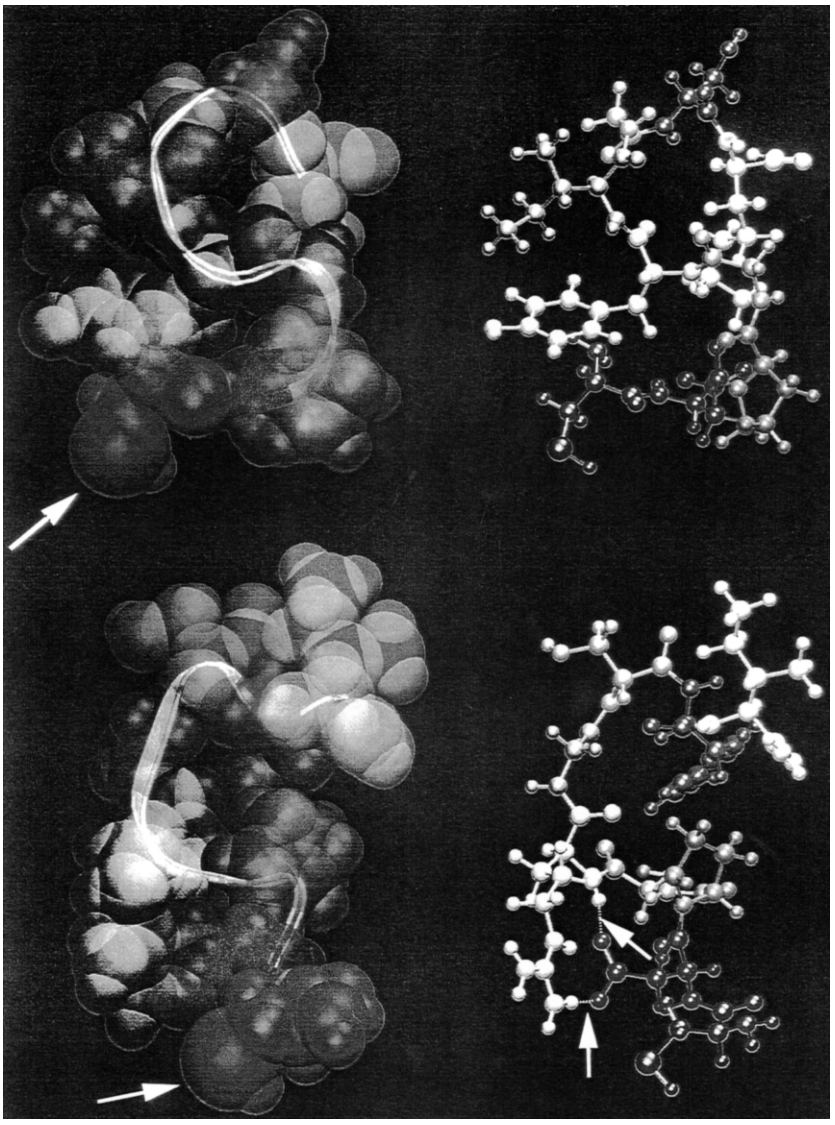

Fig. 3. H-CDPGYIGSK-NH_2 (top half) and H-CDPGRGSYI-NH_2 (bottom half) simulated in water, with the superposition of the backbone structures on the space-filling models shown on the left hand side, and the ball-and-stick models shown on the right hand side. The occurrence of single H-bonds in H-CDPGRGSYI-NH_2 is indicated with the yellow arrows, whereas in H-CDPGYIGSK-NH_2 they occur with such low frequency or too transient to be captured. Note that the sulfurs (white arrows) of the Cys are also exposed. Graphics obtained with VMD package [31].

of gyration in the range of 5.7–6.2 Å and an average end-to-end distance of approximately 12 Å; therefore, implying that immobilizing the peptide via its cysteine terminus did not affect its overall structure (Fig. 2, bottom). The scrambled peptide had similar dimensions as H-CDPGYIGSR-NH_2, but exhibited a much greater tendency to fluctuate around the average value, suggesting that its structure was very mobile and less defined than the other peptides. The H-CDPGYIGSK-NH_2 displayed a similar end-to-end distance, but a lower average radius of gyration (5.3 Å) in comparison to the other peptides.

Fig. 4 shows a histogram plot obtained from the

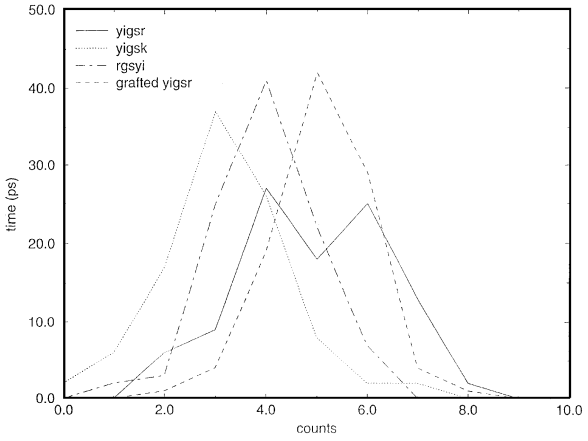

Fig. 4. Graph showing frequency of H-bonding within each of the peptide systems simulated in water. Note that peaks for both free-floating and grafted H-CDPGYIGSR-NH_2 are shifted to the right relative to the others, indicative of higher H-bonding activity.

analysis of H-bond formation for the four systems. The histograms of both the free and grafted H-CDPGYIGSR-NH_2 systems are shifted to the right, indicating a greater tendency for these systems towards the formation of intramolecular H-bonds, in accordance with the earlier findings in vacuum for free H-CDPGYIGSR-NH_2. The free and grafted H-CDPGYIGSR-NH_2 systems also have histograms centered around the same mean value. The scrambled peptide, on the other hand, shows a tendency that is intermediate between the H-CDPGYIGSR-NH_2 systems and H-CDPGYIGSK-NH_2.

By looking in detail at the most stable H-bonds, i.e. the most frequently occurring intramolecular H-bonds during the simulations, we obtain the results reported in Table 1. From the table, it is evident that H-CDPGYIGSR-NH_2 has similar H-bond patterns in both the free and grafted conditions. The Arg–Asp H-bond pattern, as previously observed in vacuum, has a dominant role in stabilizing the peptide conformation. The H-CDPGYIGSR-NH_2 structure is mostly stabilized by intramolecular H-bonds and by the central Gly residue that adopts a bending conformation. The Arg and Asp groups of H-CDPGYIGSR-NH_2, by virtue of each having a pair of donor and acceptor atoms, form intramolecular H-bonds that are

Table 1
A comparative tabulation of the number of intramolecular H-bonds occurring between the atoms of the indicated residues of the various peptides[a]

	CDPGYIGSR			
Atomic pairs	free H-CDPGYIGSR-NH_2	Grafted H-CDPGYIGSR-NH_2		
$(N)_{Gly}$–$(O\gamma_2)_{Asp}$	1797	1890		
$(N)_{Tyr}$–$(O)_{Pro}$	628	282		
$(N)_{Arg}$–$(O)_{Gly}$	1491	1987		
$(N)_{Arg}$–$(O_\beta)_{Ser}$	108	–		
$(N_\delta)_{Arg}$–$(O_\beta)_{Ser}$	249	–		
$(N_{\varepsilon*})_{Arg}$–$(O_{\gamma*})_{Asp}$	7354	7577		
CDPGYIGSK		CDPGRGSYI		
Atomic pairs	free H-CDPGYIGSK-NH_2	Atomic pairs	free H-CDPGRGSYI-NH_2	
$(N_\varepsilon)_{Lys}$–$(O_{\gamma*})_{Asp}$	2556	$(N_{\varepsilon*})_{Arg}$–$(O_{\gamma*})_{Asp}$	3683	
$(N_\varepsilon)_{Lys}$–$(O)_{Asp}$	1655	$(N)_{Arg}$–$(O_{\gamma*})_{Asp}$	2367	
$(N_\varepsilon)_{Lys}$–$(O)_{Tyr}$	1233	$(N_\delta)_{Arg}$–$(O_{\gamma*})_{Asp}$	3701	
$(N_\varepsilon)_{Lys}$–$(O_\beta)_{Ser}$	1025			
$(N)_{Tyr}$–$(O)_{Asp}$	584			
$(N)_{Tyr}$–$(O)_{Pro}$	1877			

[a] H-bonds are counted whenever the donor-acceptor distance is less than 3.5 Å, and the angle between H donor-acceptor is between 115 and 245°. The table reports only the most frequently occurring H-bonds during analysis of 2500 configurations. Greek letter subscripts refer to the sequential position of the side-chain carbon relative to the backbone carbon. Subscripts are omitted for atoms from the backbone carbon, and asterisks indicate all possible such atoms at the indicated sequential position.

practically unbroken during the whole simulation run. On the contrary, the H-CDPGYIGSK-NH_2 and scrambled peptides do not have multiple H-bond acceptors in their terminal residues. Therefore, the mutation of Arg to Lys significantly alters intramolecular H-bonding pattern, thereby impacting on overall peptide conformation.

The 0 K protocol applied to the H-CDPGYIGSR-NH_2 systems supports the results discussed above. It revealed that over the five different quenching cycles carried out, three of the five minimized structures having lower potential energies of −142, −114 and −100 kcal/mol form intramolecular Asp–Arg H-bonds, a double bond in the first case and single bonds in the two other cases. The remaining two structures, with potential energies of −92 and −81 kcal/mol, also retain the same Arg–Asp H-bond. However, additional H-bonds, in particular for Ser–Ile, Arg–Ser, and Gly–Asp, were also seen for these cases. Nevertheless, the Gly dihedral conformation and general H-bond network has a very similar behavior, as observed dynamically and with the MSDS analysis earlier.

3.3. Surface characterization with ESCA

The chemical formula of the oligopeptides H-CDPGYIGSR-NH_2 and H-CDPGRGSYI-NH_2 is $C_{40}H_{64}O_{13}N_{13}S$, and for H-CDPGYIGSK-$NH_2$, $C_{40}H_{63}O_{13}N_{11}S$. An ESCA study of the plain (unmodified) gold substrates detected typically three elements, i.e. gold, carbon and oxygen. It is presumed that the latter elements (C and O) are related to adventitious ambient contamination. An ESCA of the peptide-modified substrates demonstrated the additional presence of nitrogen at a binding energy of approximately 400 eV. Sulfur could not be detected. Table 2 summarizes the elemental composition of the modified and unmodified substrates, together with their relative surface concentrations. The stoichiometric composition of the peptide (shown in line 5 of Table 2) shows a theoretical N/O ratio of 0.86, which compares well with the experimental value on peptide-modified surfaces of 0.88 (line 2), suggesting that the oxygen observed on the peptide-modified gold surface is primarily related to the peptide rather than contamination. It has indeed been previously reported that organosulfur compounds typically displace organic contaminants on gold surfaces [32]. The theoretical N/C ratio is 0.30, and thus, for an experimental value of 11.7% nitrogen, the expected value of peptide-related carbon should be approximately 39%. However, the experimental value is 62.6%, with the additional 23.6% probably related to irreversible hydrocarbon contamination. Given that carbon is the elemental backbone of the peptide, information about its chemical bonding could shed more light on the nature of the compound present on the surface. The decomposition of the C 1s peak resulted in three major component peaks at binding energies of 285.1, 286.7 and 288.5 eV (Fig. 5), which were primarily associated with the presence of $-CH_2-CH_2-$ (285 eV), C–OH or $-CH_2-N$ (286.7 eV) and N–C=O (288 eV), which are all typical of residues found in amino acids and are also in agreement with previous reports on ESCA analysis of immobilized peptides [11].

Table 2
Relative surface concentrations of the various elements detected with ESCA on gold substrates modified with CDPGYIGSR (denoted -YIGSR), CDPGYIGSK (denoted -YIGSK) and CDPGRGSYI (denoted -RGSYI) oligopeptides[a]

Sample type	%C	%O	%N	%Au
Au-Unmodified	56.0	7.1	0.9	35.9
Au-YIGSR	62.6	13.3	11.7	12.4
Au-YIGSK	61.6	11.3	9.0	18.1
Au-RGSYI	61.1	13.7	11.8	13.4
YIGSR (Theoretical)	59.7	20.9	17.9	

[a] The last row gives the theoretical elemental composition of the CDPGYIGSR oligopeptide. Note the exclusive presence of nitrogen on peptide-modified surfaces vs. the unmodified one.

3.4. Biological assays

Peptide-modified surfaces were subsequently tested for their capability to elicit the appropriate bioresponse on NG108-15 cells, a cell line documented to be capable of highly specific interactions with the H-CDPGYIGSR-NH_2 minimal peptide sequence during cell adhesion events. Af-

ter 4 h in culture in serum-containing media, good attachment of NG108 cells could be observed on H-CDPGYIGSR-NH_2 surfaces, with cells typically displaying a flattened and spreading morphology (Fig. 6a). On the contrary, there was barely any attachment on unmodified gold surfaces at this point; cells typically required more time to attach on unmodified gold in serum conditions (Fig. 6b). Quantification of these observations revealed that cell adhesion levels were indeed significantly enhanced on H-CDPGYIGSR-NH_2 surfaces vs. unmodified surfaces (Fig. 7a). In addition, there were more cells extending processes or neurites on H-CDPGYIGSR-NH_2 than on unmodified surfaces (data not shown). However, if the cells were first incubated in a medium also containing soluble H-CDPGYIGSR-NH_2 peptide prior to being cultured in serum-free media on surfaces modified with H-CDPGYIGSR-NH_2, lower levels of cell attachment resulted, decreasing down to comparable levels or even below what is seen on unmodified surfaces (Fig. 7b). A comparison of cell attachment levels between H-CDPGYIGSK-NH_2 and H-CDPGYIGSR-NH_2 surfaces in serum-free media showed a decrease on H-CDPGYIGSK-NH_2 surfaces to approximately the same levels as unmodified surfaces (Fig. 7c).

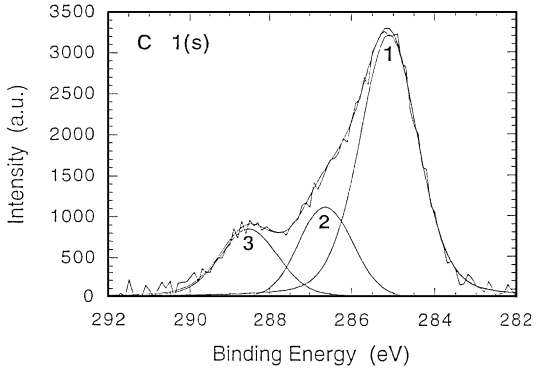

Fig. 5. Deconvoluted carbon peak (C1s) on gold substrate modified with H-CDPGYIGSR-NH_2, showing the surface presence of peptide related species at binding energies of 286.5 and 288.3 eV. Curve 1 indicates presence of hydrocarbon contributions, curve 2 indicates presence of C–OH and CH_2–N, and curve 3 is associated with N–C=O functional groups.

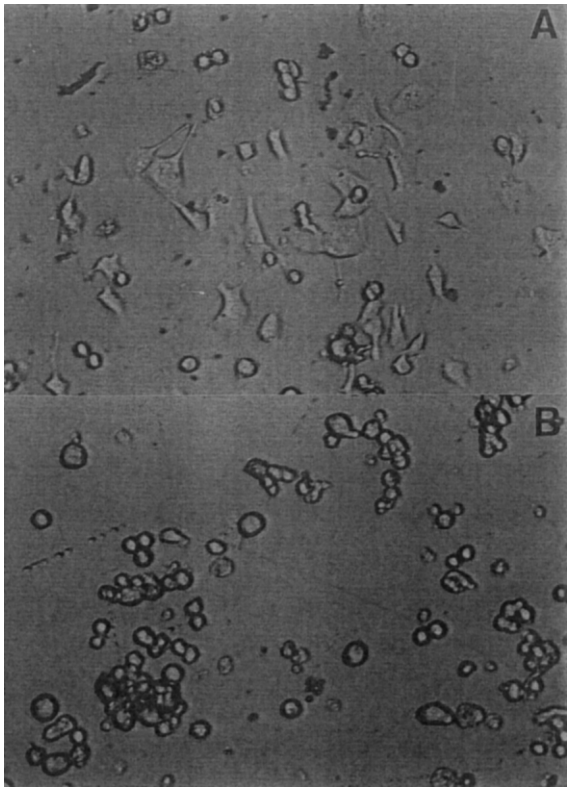

Fig. 6. A micrograph of NG108-15 cells on gold surfaces modified with the attachment-promoting oligopeptide, H-CDPGYIGSR-NH_2, after 4 h in serum-containing culture conditions. Note the prevalence of good cell attachment (Fig. 6a). On the contrary, unmodified gold displays poor or no cell attachment at this time point (Fig. 6b). Magnification is 250 ×.

4. Discussion

In this study, an in-depth molecular characterization of the laminin-derived oligopeptide H-CDPGYIGSR-NH_2 was carried out using molecular dynamics simulations. We also examined various other parameters not considered in previous studies, but deemed essential for a more in depth understanding of peptide structure. These included the behavior of peptide structure in an aqueous environment, or in an immobilized state, i.e. with one end (cysteine terminus) immobilized. To gain additional insight, a comparative study of variants or analogs of the oligopeptide was also

carried out. Inspired by the results predicted by the simulations, an in vitro model was implemented to corroborate and assist in the interpretation of the simulated results.

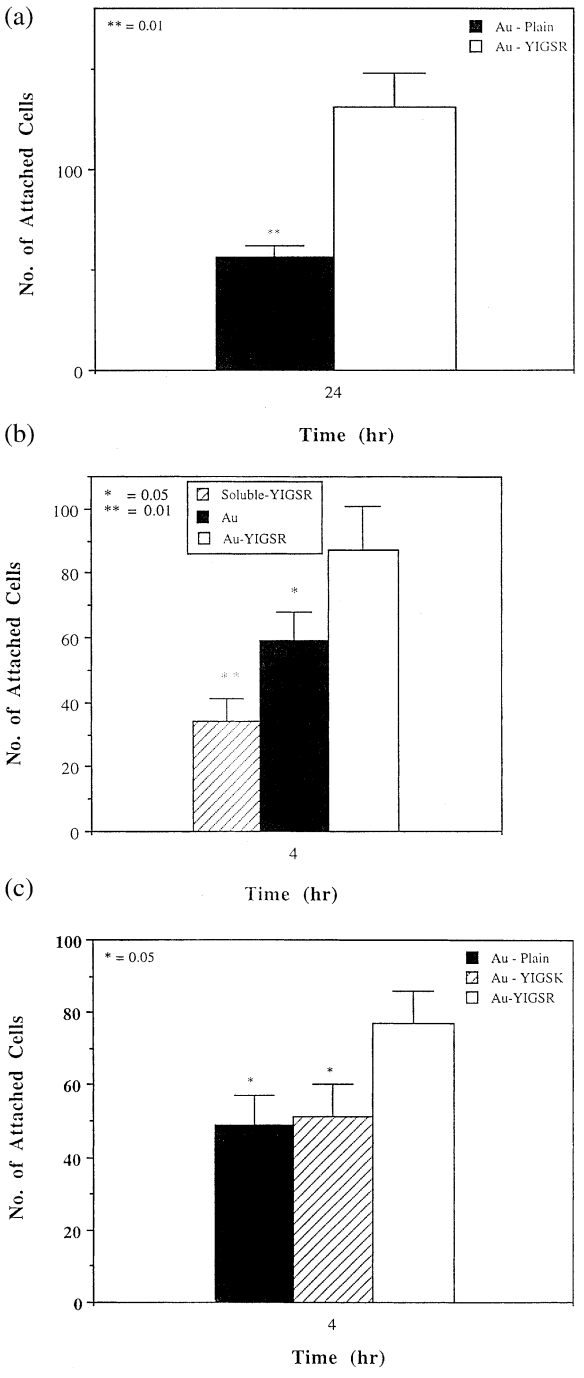

Fig. 7.

4.1. Molecular dynamics structure of oligopeptides

The replacement of the terminal arginine residue (in CDPGYIGSR) with a lysine residue leads to a significant change in peptide structure and stability, even though these residues have relatively similar properties, i.e. they are both hydrophilic and positively charged at physiological pH. This structural discrepancy is attributed to the predominant presence of a relatively stable double hydrogen bond for CDPGYIGSR between arginine and aspartic acid, whereas in the case of CDPGYIGSK, the predominant intramolecular hydrogen bond is a single bond between lysine and serine. We believe that the Arg–Asp double H-bond in CDPGYIGSR is what primarily confers the overall structure to this peptide. Since double bonds are generally known to hinder torsional motion, the effect of this on the terminal Arg might be to constrain its rotational mobility, thereby probably stabilizing and improving its optimal presentation. In CDPGYIGSK, the predominant or the most stable intramolecular bond is a single bond (Lys–Ser), which is generally more permissive to rotational mobility than the double bond. Therefore, the marked mobility observed for the Lys side chain might probably be a consequence of the rotational mobility permitted in this case, whose net effect would be to decrease the probability of finding it in a particular (and perhaps optimal) configuration. Intrinsic peptide fluctuations, as determined from the end-to-end vectors and radii of gyration, are believed to be generally less significant contributing factors in our observed peptide structures. In both

Fig. 7. Histogram showing NG108 cell attachment densities on unmodifed and YIGSR-modified gold surfaces in serum-containing media (Fig. 7a). The vertical scale denotes the average number of attached cells per mm^2. Fig. 7b shows competitive binding assays on the YIGSR-modified surfaces in serum-free media. Fig. 7c shows cell attachment densities on YIGSR and YIGSK-modified gold surfaces in serum-free media. Note that YIGSR and YIGSK denote H-CDPGYIGSR-NH_2 and H-CDPGYIGSK-NH_2, respectively.

peptides, however, the cysteine residues and their sulfhydryl groups are freely exposed, meaning that they may be available to appropriate target interactions in their environment. Furthermore, similar results were obtained when peptides were studied in a solvated/water medium, even though peptide structures are slightly less stable here. This is particularly significant, as water is known to be a very keen competitor for hydrogen bonding and, therefore, poses a potential danger of disrupting the previously observed peptide structure. It may, therefore, be reasonable to suggest that a similar peptide structure for CDPGYIGSR would be expected under physiological conditions as well.

It has been previously reported that the pentapeptide YIGSR-NH_2 alone displays an almost similar, but slightly less potent, bioactivity than the nonapeptide CDPGYIGSR-NH_2, leading to the conclusion that the pentapeptide represents the minimal sequence required for efficient bioactivity [5]. Nevertheless, while the nonapeptide may derive most of its bioactivity from the upper five terminal residues (YIGSR), the presence of the lower terminal residues (CDPG) still seems to augment the peptide's bioactivity. On the basis of the involvement of the Asp residue in the predominant Asp–Arg double H-bond in CDPGYIGSR from the simulation studies, it would be expected that variation of the Asp residue in CDPG would probably affect the bioactivity of the peptide. Indeed the work of Ranieri et al. [11] seems to partially support this hypothesis. They observed diminished peptide bioactivity when GGGGYIGSR was used instead of CDPGYIGSR, therefore raising the possibility that the bottom terminal residues may not simply serve to tether the peptide, but probably contribute to its bioactivity in other ways as well. The simulation results, therefore, provide possible clarification of the role of the terminal residues in CDPGYIGSR, in that they implicate a major contribution of at least one of the residues (Asp) in stabilizing peptide structure. It might be enlightening in the future to check this hypothesis further by studying the outcome of mutating Asp with Glu, since these amino acids are otherwise similar with the exception of an extra methyl group in Glu.

4.2. Surface immobilization of oligopeptides

The surface chemical information derived from ESCA revealed the presence of peptide-related species on all the peptide-modified surfaces, thus strongly suggesting peptide presence on these surfaces. Since nitrogen was observed exclusively on peptide-modified surfaces, it was chosen as the marker for assessing peptide incorporation. ESCA reported nitrogen surface concentrations of approximately 12% for both H-CDPGYIGSR-NH_2 and H-CDPGRGSYI-NH_2 surfaces, and approximately 9% for the H-CDPGYIGSK-NH_2 surface. The H-CDPGYIGSR-NH_2 and H-CDPGRGSYI-NH_2 peptides have identical residues with each containing approximately 13 nitrogen atoms per molecule, whereas the H-CDPGYIGSK-NH_2 molecule has approximately 11 nitrogen atoms, as lysine (K) has fewer nitrogens than arginine (R). Therefore, the relative nitrogen proportions of the various oligopeptides as determined with ESCA are in reasonable agreement with theoretical expectations. These observations are also reinforced by a recent investigation where a similar peptide was deposited on a composite biochip surface consisting of Teflon-AF, gold and oxidized silicon. Using time-of-flight secondary ion mass spectroscopy, it was shown that the peptide only incorporated in the gold micro domains of the biochip surface [33]. Successful incorporation of the peptides on gold surfaces would indeed be a reinforcement of the predictions of the simulations, which predicted the availability of the sulfhydryl side chain of the terminal cysteine. Since gold is otherwise inert, the only mechanism by which the peptide can incorporate under these conditions is via the sulfhydryl group.

4.3. Bioactivity of immobilized oligopeptides

The marked increase in cell adhesion observed on YIGSR-modified surfaces indicates that the

NG108-15 cells have a high affinity for this surface. This phenomenon, however, is reversed or neutralized if the cells are pre-incubated in media containing the soluble peptide, as seen with the competitive binding experiments. A plausible explanation for this reversal could relate to the fact that the soluble peptide in the media possibly binds to the appropriate cell's surface receptors during the pre-incubation. If the higher affinity for the YIGSR surfaces observed before is indeed receptor mediated, most of these receptors would be saturated or quenched after the pre-incubation stage and, therefore, would no longer be available to participate in subsequent cell adhesion events, thereby accounting for the decrease in cell attachment levels seen in the competitive assays. While we have not specifically demonstrated receptor engagement per se, we feel that these results strongly implicate receptor involvement in the cell attachment events on the YIGSR surfaces. Altogether, these data suggest that not only is the peptide bound, but that it also retains its expected bioactivity under these conditions. The absence of enhancement of cell adhesion with H-CDPGYISGK-NH_2 surfaces suggest an element of specificity with H-CDPGYIGSR-NH_2 substrates, thereby lending additional support to our conclusion.

The kinetics of cell attachment on unmodified gold tended to differ between serum-containing and serum-free media conditions. In serum-free conditions, cell attachment typically occurred more rapidly than serum-containing conditions. This could probably be attributed partly to the fact that the gold surfaces are slightly hydrophobic and, therefore, in the presence of the serum protein albumin, may resist cell attachment initially, until other attachment-promoting serum proteins, like fibronectin, are eventually deposited by competitive protein desorption. However, this problem seems to be resolved if the gold surface is modified with the attachment-promoting H-CDPGYIGSR-NH_2 oligopeptide, even though no appreciable difference is observed in the contact angles of the modified and unmodified surfaces.

5. Conclusion

In summary, molecular dynamics simulation and corresponding experimental studies of the laminin-derived oligopeptide H-CDPGYIGSR-NH_2 were carried out. The oligopeptide structure obtained from the simulations was essentially in agreement with that previously reported under similar (vacuum) conditions. The present study included the treatment of additional important parameters, i.e. the behavior of the peptide structure in an aqueous medium, and a peptide simulation with one end of the peptide immobilized. In both these conditions, the overall peptide structure observed closely resembled the one observed in the vacuum medium, prompting us to believe that this may indeed be the peptide structure most likely to occur under physiological conditions. Intramolecular hydrogen bonding analysis revealed that the observed peptide structure was primarily due to a relatively stable, predominant double hydrogen bond between the arginine (R) and aspartic acid (D) residues.

The drastic structural change observed after the replacement of the terminal arginine (R) with lysine (K) may help to explain the attenuation or abolishment of the oligopeptide's bioactivity observed experimentally. This structural difference is attributed to marked changes in the intramolecular hydrogen bonding pattern predicted by the simulations upon effecting the mutation.

A contribution of the aspartic acid residue in the overall oligopeptide structure is implicated via its participation in the predominant Arg–Asp double hydrogen bond, thus revealing a possible major role for one of the residues in the CDPG amino acid sequence, whose role had previously been unconfirmed, and sometimes suggested to be redundant.

It is hoped that the computational/experimental tandem-approach adopted herein may find further utility in the design of future ligand/receptor studies, and that these results may also be of value in the domains of biosensors, biomaterials and tissue engineering.

6. Abbreviations

C	Cysteine
D	Aspartic acid
P	Proline
G	Glycine
Y	Tyrosine
I	Isoleucine
S	Serine
R	Arginine
K	Lysine
A	Alanine
V	Valine
ESCA	Electron spectroscopy for chemical analysis
SPME	Smooth particle mesh Ewald
MSDS	Most stable dynamical structure

Acknowledgements

We thank Dr Maddalena Venturoli for assistance during the setting-up of the simulations. ESCA analysis was performed by Nicolas Xanthapoulos in Professor Hans Jorg Mathieus Surface Analysis Group at the Swiss Federal Institute of Technology in Lausanne. This work was supported by the Swiss Priority Program in Materials (module 4.2A).

References

[1] H.K. Kleinman, G.C. Sephel, K.-I. Tashiro et al., Laminin in neuronal development, Ann. NY Acad. Sci. 580 (1990) 302–310.

[2] P.C. Letourneau, L.C. Condic, D.M. Snow, Interactions of developing neurons with the extracellular-matrix, J. Neurosci. 14 (1994) 915–928.

[3] L. McKerracher, M. Chamoux, C.O. Arregui, Role of laminin and integrin interaction in growth cone guidance, Mol. Neurobiol. 12 (1996) 95–116.

[4] J. Graf, Y. Iwamoto, M. Sasaki et al., Identification of an amino-acid sequence in laminin mediating cell attachment, chemotaxis, and receptor-binding, Cell 48 (1987) 989–996.

[5] J. Graf, R.C. Ogle, F.A. Robey et al., A pentapeptide from the laminin-β1 chain mediates cell-adhesion and binds the 67000-laminin receptor, Biochemistry 26 (1987) 6896–6900.

[6] K. Tashiro, G.C. Sephel, B. Weeks et al., A synthetic peptide containing the IKVAV sequence from the α-chain of laminin mediates cell attachment, migration, and neurite outgrowth, J. Biol. Chem. 264 (1989) 16174–16182.

[7] J.B. McCarthy, A.P. Skubitz, S.L. Palm, L.T. Furcht, Metastasis inhibition of different tumor types by purified laminin fragments and a heparin-binding fragment of fibronectin, J. Nat. Cancer Inst. 80 (1988) 108–116.

[8] M. Zhao, H. Kleinman, M. Mokotoff, Synthetic laminin-like peptides and pseudopeptides as potential antimetastatic agents, J. Med. Chem. 37 (1994) 3383–3388.

[9] Y. Kaneda, S. Yamamoto, T. Kihira et al., Cell-adhesive laminin peptide YIGSR conjugated with polyethylene glycol has improved antimetastatic activity due to a longer half-life in blood, Invasion Metastasis 15 (1995) 156–162.

[10] J.F. Clémence, J.P. Ranieri, P. Aebischer, H. Sigrist, Photoimmobilization of a bioactive laminin fragment and pattern-guided selective neuronal cell attachment, Bioconjugate Chem. 6 (1995) 411–417.

[11] J.P. Ranieri, R. Bellamkonda, J.B. Bekos et al., Spatial control of neuronal cell attachment and differentiation on covalently patterned laminin oligopeptide substrates, Int. J. Devl. Neurosci. 12 (1994) 725–735.

[12] J.P. Ranieri, R. Bellamkonda, J.B. Bekos, T.G. Vargo, J.A. Gardella, P. Aebisher, Neuronal cell attachment to fluorinated ethylene-propylene films with covalently immobilized laminin oligopeptides YIGSR and IKVAV.2., J. Biomed. Mater. Res. 29 (1995) 779–785.

[13] S.P. Massia, S.S. Rao, J.A. Hubbell, Covalently immobilized laminin peptide TYR-ILE-GLY-SER-ARG (YIGSR) supports cell spreading and colocalization of the 67-Kdalton laminin receptor with alpha-actinin and vinculin, J. Biol. Chem. 268 (1993) 8053–8059.

[14] S.P. Massia, J.A. Hubbell, Covalent surface immobilization of ARG-GLY-ASP-containing and TYR-ILE-GLY-SER-ARG-containing peptides to obtain well-defined cell-adhesive substrates, Anal. Biochem. 187 (1990) 292–301.

[15] M. Borkenhagen, J.F. Clémence, H. Sigrist, P. Aebischer, Three-dimensional extracellular matrix engineering in the nervous system, J. Biomed. Mater. Res. 40 (1998) 392–400.

[16] P.W. Brandt-Rauf, M.R. Pincus, R.P. Carty et al., Conformation of the metastasis-inhibiting laminim pentapeptide, J. Protein Chem. 8 (1989) 149–157.

[17] D.R. McKelvey, C.L. Brooks, M. Mokotoff, A Charmm analysis of the conformations of the metastatis-inhibiting laminin pentapeptide, J. Protein Chem. 267 (1991) 25120–25128.

[18] G.J. Ostheimer, J.R. Starkey, C.G. Lambert, S.L. Helgerson, E.A. Dratz, NMR constrained solution structures for laminin peptide-11 analogs define structural requirements for inhibition of tumor-cell invasion of basement-membrane matrix, J. Biol. Chem. 267 (1992) 25120–25128.

[19] C.D. Bain, E.B. Troughton, Y.-T. Tao, J. Evall, G.M. Whitesides, R.G. Nuzzo, Formation of monolayers films

by the spontaneous assembly of organic thiols from solution onto gold, J. Am. Chem. Soc. 111 (1989) 321–335.
[20] D.T. Clark, ESCA applied to polymers, Adv. Polym. Sci. 24 (1977) 125–188.
[21] DLPOLY is a package of molecular simulation routines written by Smith, W., Forester, T.R., copyright, The Council for the Central Laboratory of the Research Council, Daresbury Laboratory, Daresbury, Nr. Warrington (1996). DLPROTEIN was developed from DLPOLY for the simulation of proteins at the Italian Institute for the Physics of Matter, under the network on 'Molecular dynamics simulation of biosystems' (1997).
[22] S. Melchionna, S. Cozzini, DLPROTEIN 1.2 User Manual, University of Rome, 1997.
[23] B.R. Brooks, R.E. Bruccoleri, B.D. Olafson, D.J. States, S. Swaminathan, M. Karplus, Charmm — a program for macromolecular energy, minimization, and dynamics calculations, J. Comp. Chem. 4 (1983) 187–217.
[24] G. Ciccotti, J.-P. Ryckaert, Molecular dynamics simulation of rigid molecules, Comp. Phys. Rep. 4 (1986) 345–392.
[25] W.L. Jorgensen, J. Chandrasekhar, J.D. Madura, R.W. Impey, M.L. Klein, Comparison of simple potential functions for simulating liquid water, J. Chem. Phys. 79 (1983) 926–935.
[26] M.P. Allen, D.J. Tildesley, Computer Simulation of Liquids, Clarendon Press, Oxford, 1987.
[27] E. Essmann, L. Perera, M.L. Berkowitz, T. Darden, H. Lee, L.J. Pedersen, A smooth particle mesh Ewald, J. Chem. Phys. 103 (1995) 8577–8593.
[28] S. Melchionna, G. Ciccotti, B.L. Holian, Hoover NpT dynamics for systems varying in shape and size, Mol. Phys. 78 (1993) 533–544.
[29] C.L. Brooks, M. Karplus, B.M. Pettitt, in: I. Prigogine, S.A. Rice (Eds.), Advances in Chemical Physics, 71, John Wiley and Sons, New York, 1988.
[30] L. Stella, S. Melchionna, Equilibration and sampling in molecular dynamics simulations of biomolecules, J. Chem. Phys. 109 (1998) 10115.
[31] W. Humphrey, A. Dalke, K. Schulten, VMD: visual molecular dynamics, J. Mol. Graphics 14 (1996) 33–38.
[32] E.B. Troughton, C.D. Bain, G.M. Whitesides, R.G. Nuzzo, D.L. Allara, M.D. Porter, Monolayer films prepared by the spontaneous self-assembly of symmetrical and unsymmetrical dialkyl sulfides from solution onto gold substrates-structure, properties, and reactivity of constituent functional groups, Langmuir 4 (1988) 365.
[33] S.A. Makohliso, D. Léonard, L. Giovangrandi, H.J. Mathieu, M. Ilegems, P. Aebischer, Surface characterization of a biochip prototype for cell-based biosensor applications, Langmuir 15 (1999) 8552.